Supporting information

Extraordinary Electromechanical Actuation of Ti_2C MXene

Bozhao Wu, Xiaoxi Cai, Langquan Shui, Enlai Gao* and Ze Liu

Department of Engineering Mechanics, School of Civil Engineering, Wuhan University, Wuhan, Hubei 430072, China.

*Corresponding author. E-mail: enlaigao@whu.edu.cn

This supporting information contains

(1) Sections 1-2.

(2) Figures S1-S6.

(3) Table S1.

(4) Movie S1.

Section 1: Calculations of actuation performance

(1) Actuation strain

The actuation strain of Ti_2C MXene upon charge injection along the armchair (*x* direction) or zigzag (*y* direction) direction is defined as:

$$\varepsilon_x = \frac{a - a_0}{a_0}, \varepsilon_y = \frac{b - b_0}{b_0} \tag{1}$$

where a_0 and b_0 are lattice constants of pristine Ti_2C MXene, a and b are the lattice constants of Ti_2C MXene upon charge injection, respectively. Figure 2a shows the actuation strain of Ti_2C MXene upon charge injection as compared with other 2D materials (Figure S1a).

(2) Areal actuation expansion

As shown in Figure 2a, the charged Ti_2C MXene shows the same actuation strain along the armchair and zigzag directions. The areal actuation expansion (S_ε) of the charged Ti_2C MXene is characterized by the following formula:

$$S_\varepsilon = \frac{ab - a_0 b_0}{a_0 b_0} \tag{2}$$

Eq. (2) can be rewritten as:

$$S_\varepsilon = (\varepsilon_x + 1)(\varepsilon_y + 1) - 1 \tag{3}$$

The calculated S_ε was shown in Figure 2a. Besides, according to the data in Figure S1a, the areal actuation expansions of graphene, silicene and black phosphorene (BP) were also determined for the comparison with that of Ti_2C monolayer (Figure S1b).

Section 2: Calculation of gravimetric work densities

The gravimetric work densities (W_g) for 2D materials are usually defined as[1]:

$$W_g = \frac{S\varepsilon_{max}^2}{2\rho} \tag{4}$$

where ε_{max} is the maximum actuation strain upon charge injection, S is the in-plane stiffness and ρ is the areal density of 2D materials. Considering the significant actuation strain both along the zigzag and armchair directions of Ti_2C MXene, the total gravimetric work density should be contributed from both armchair and zigzag directions:

$$W_{vol} = W_{g,\ armchair} + W_{g,\ zigzag} \tag{5}$$

Additionally, previous work demonstrated that the in-plane stiffness of charged phosphorene would remarkably reduce upon hole injection[2]. As shown in Figure S3a, the in-plane stiffnesses of hole charged Ti_2C monolayer also show a reduction with the increase of hole injection. To address this issue, a realistic gravimetric work density ($W_{g\text{-}r}$) is defined as[2]

$$W_{g\text{-}r} = \frac{1}{2\rho}\int \sigma_i d\varepsilon_i \tag{6}$$

The total realistic gravimetric work densities are written as

$$W_{g\text{-}r} = W_{g\text{-}r,\ armchair} + W_{g\text{-}r,\ zigzag} \tag{7}$$

The calculated realistic work densities ($W_{g\text{-}r}$) are shown in Figure S3b.

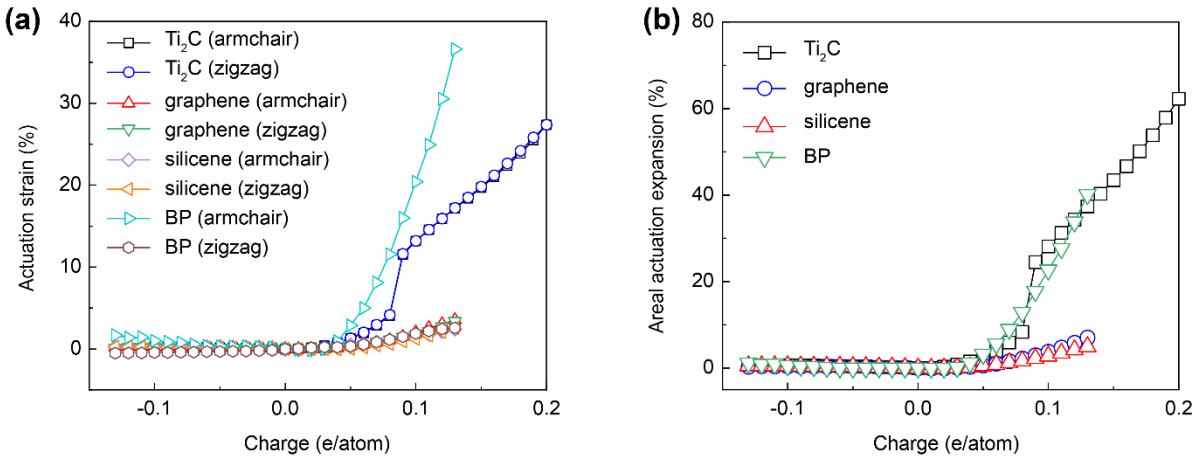

Figure S1. (a) Actuation strain and (b) areal actuation expansion of Ti_2C MXene upon charge injection, as compared with graphene, silicene and black phosphorene (BP) monolayer. The data of graphene, silicene and BP was adopted from the **Ref**[2].

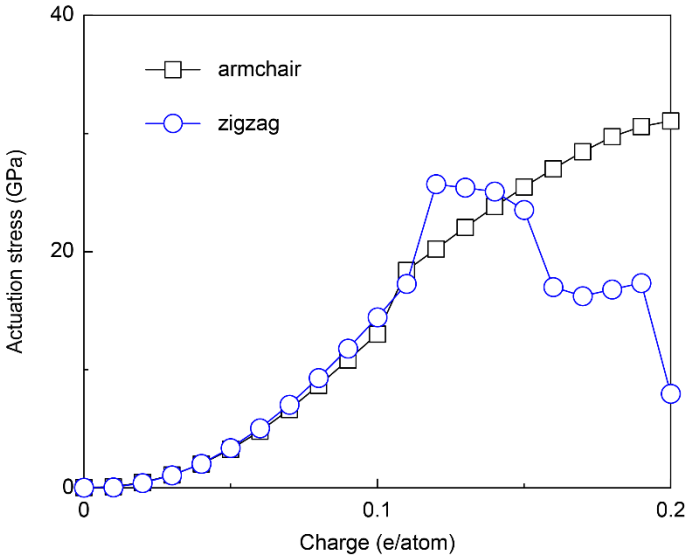

Figure S2. Uniaxial actuation stress of Ti_2C MXene upon charge injection.

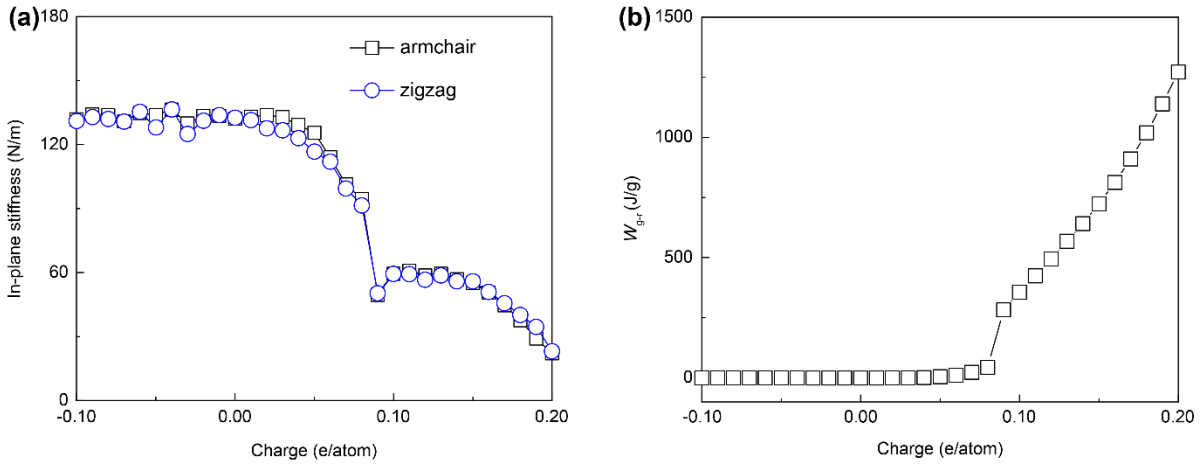

Figure S3. (a) In-plane stiffnesses of the charged Ti_2C MXene along the armchair and zigzag directions. (b) Realistic gravimetric work densities ($W_{g\text{-}r}$) of Ti_2C MXene.

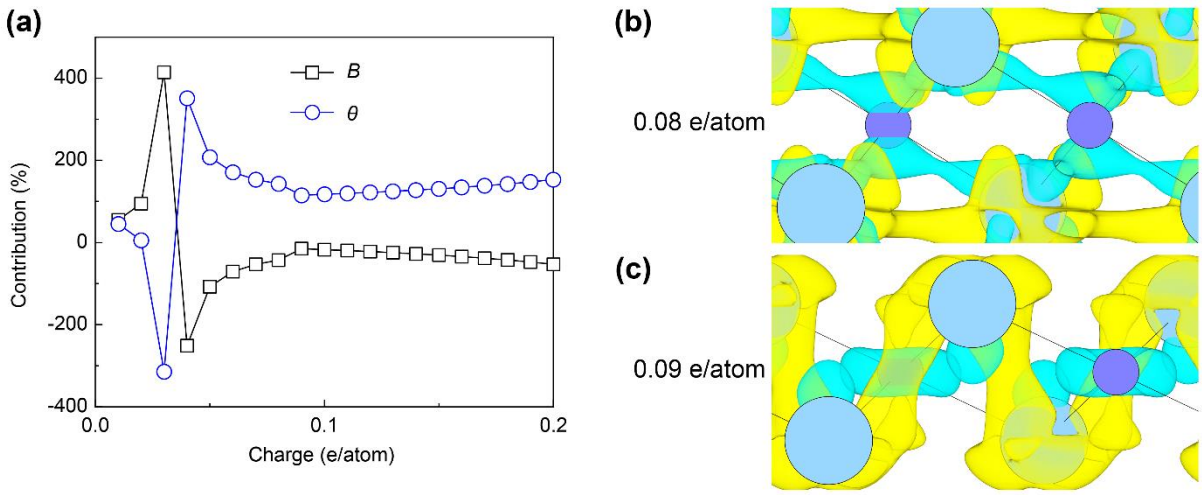

Figure S4. (a) Contributions of internal bond (B) and bond angle (θ) on the interlayer thickness ($d_{\text{Ti-Ti}}$) for Ti_2C MXene. The partial zoom of the excess charge density distributions of Ti_2C MXene upon (b) 0.08 and (c) 0.09 e/atom injection with an iso-surface value of 0.0005 e/Bohr^3.

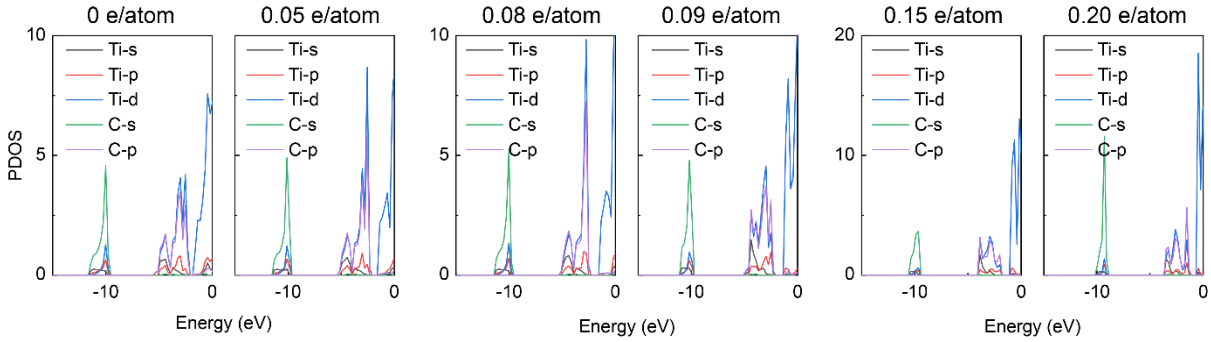

Figure S5. Projected density of state (PDOS) of the charged Ti_2C MXene upon hole injection of 0.05, 0.08, 0.09, 0.15 and 0.20 e/atom as compared with pristine Ti_2C MXene.

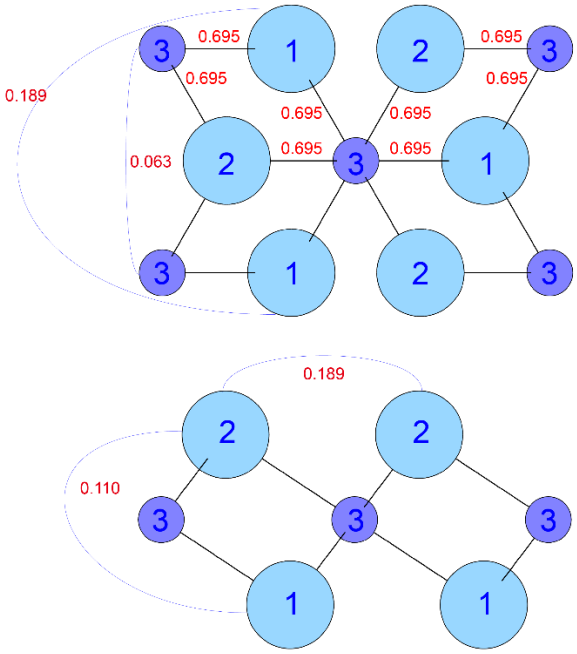

Figure S6. Bond orders (BOs) for different bond pairs (Ti-C, C-C and Ti-Ti) of the pristine Ti_2C MXene calculated by using DDEC6 atomic population analysis[3].

Table S1 Summary of maximum actuation strain ε_{max} (%) and gravimetric work density W_g (J/g) of typical actuation materials.

Type	Materials name	ε_{max}	W_g
Traditional materials	Natural muscle[4]	40	0.0386
	Magnetostrictor[5]	0.2	0.0216
	PZN-PT single crystal[6]	1.7	0.131
	Polyurethane elastomer[7]	4	0.013
	P(VDF-TrFE)[8]	4	0.16
	Polyaniline yarn[9]	0.28	0.0056
Metal	Pd rod[10]	3.3	1.27
	Au-Pt alloy rod[11]	1.3	0.4
2D materials	CNT aerogel sheets[12]	1.5	0.03
	CNT buckypaper[1]	1	24
	Coiled graphene/CNT yarn[13]	19.4	2.6
	Coiled CNT/rGO yarn[14]	8.1	0.236
	CNT@nylon6 SRAM[15]	4.7	0.99
	Two-ply coiled CNT yarn[16]	16.5	2.2
	GO-C_4O-asym-unzip[17]	9.6	1022.8
	GO-C_4O-sym-clamp[18]	6.3	329.3
	1H-WTe_2[19]	2.9	18.6
	Silicene[2]	2.5	23.1
	Graphene[2, 18] 0.13 (0.15) e/atom	3.5 (4.7)	280.2 (429.4)
	Phosphorene[2]	36.6	1076.2
	Ti_2C MXene	27.4	4360.2

Movie S1

Structure changes of Ti_2C MXene upon hole injection from 0.00 to 0.20 e/atom from the top and side views.

References

1. Baughman, R. H., Carbon nanotube actuators. *Science* **1999,** *284* (5418), 1340-1344.
2. Wu, B.; Deng, H.-X.; Jia, X.; Shui, L.; Gao, E.; Liu, Z., High-performance phosphorene electromechanical actuators. *npj Computational Materials* **2020,** *6* (1), 27.
3. Manz, T. A., Introducing DDEC6 atomic population analysis: part 3. Comprehensive method to compute bond orders. *RSC Advances* **2017,** *7* (72), 45552-45581.
4. Madden, J. D. W.; Vandesteeg, N. A.; Anquetil, P. A.; Madden, P. G. A.; Takshi, A.; Pytel, R. Z.; Lafontaine, S. R.; Wieringa, P. A.; Hunter, I. W., Artificial muscle technology: Physical principles and naval prospects. *IEEE Journal of Oceanic Engineering* **2004,** *29* (3), 706-728.
5. Hathaway, K. B.; Clark, A. E., Magnetostrictive materials. *MRS Bulletin* **1993,** *18* (4), 34-41.
6. Park, S.-E.; Shrout, T. R., Ultrahigh strain and piezoelectric behavior in relaxor based ferroelectric single crystals. *Journal of Applied Physics* **1997,** *82* (4), 1804-1811.
7. Zhenyi, M.; Scheinbeim, J. I.; Lee, J. W.; Newman, B. A., High field electrostrictive response of polymers. *Journal of Polymer Science Part B: Polymer Physics* **1994,** *32* (16), 2721-2731.
8. Zhang, Q. M.; Bharti, V.; Zhao, X., Giant electrostriction and relaxor ferroelectric behavior in electron-irradiated poly(vinylidene fluoride-trifluoroethylene) copolymer. *Science* **1998,** *280* (5372), 2101-2104.
9. Lu, W.; Fadeev, A. G.; Qi, B.; Smela, E.; Mattes, B. R.; Ding, J.; Spinks, G. M.; Mazurkiewicz, J.; Zhou, D.; Wallace, G. G.; MacFarlane, D. R.; Forsyth, S. A.; Forsyth, M., Use of ionic liquids for π-conjugated polymer electrochemical devices. *Science* **2002,** *297* (5583), 983.
10. Zhang, J.; Bai, Q.; Zhang, Z., Dealloying-driven nanoporous palladium with superior electrochemical actuation performance. *Nanoscale* **2016,** *8* (13), 7287-7295.
11. Jin, H.-J.; Wang, X.-L.; Parida, S.; Wang, K.; Seo, M.; Weissmüller, J., Nanoporous Au−Pt Alloys As Large Strain Electrochemical Actuators. *Nano Letters* **2010,** *10* (1), 187-194.
12. Aliev, A. E.; Oh, J.; Kozlov, M. E.; Kuznetsov, A. A.; Fang, S.; Fonseca, A. F.; Ovalle, R.; Lima, M. D.; Haque, M. H.; Gartstein, Y. N., Giant-stroke, superelastic carbon nanotube aerogel muscles. *Science* **2009,** *323* (5921), 1575-1578.
13. Hyeon, J. S.; Park, J. W.; Baughman, R. H.; Kim, S. J., Electrochemical graphene/carbon nanotube yarn artificial muscles. *Sensors and Actuators B: Chemical* **2019,** *286*, 237-242.
14. Qiao, J.; Di, J.; Zhou, S.; Jin, K.; Zeng, S.; Li, N.; Fang, S.; Song, Y.; Li, M.; Baughman, R. H.; Li, Q., Large-stroke electrochemical carbon nanotube/graphene hybrid yarn muscles. *Small* **2018,** *14* (38), 1801883.
15. Mu, J.; Jung de Andrade, M.; Fang, S.; Wang, X.; Gao, E.; Li, N.; Kim, S. H.; Wang, H.; Hou, C.; Zhang, Q.; Zhu, M.; Qian, D.; Lu, H.; Kongahage, D.; Talebian, S.; Foroughi, J.; Spinks, G.; Kim, H.; Ware, T. H.; Sim, H. J.; Lee, D.

Y.; Jang, Y.; Kim, S. J.; Baughman, R. H., Sheath-run artificial muscles. *Science* **2019,** *365* (6449), 150-155.

16. Lee, J. A.; Li, N.; Haines, C. S.; Kim, K. J.; Lepró, X.; Ovalle-Robles, R.; Kim, S. J.; Baughman, R. H., Electrochemically powered, energy-conserving carbon nanotube artificial muscles. *Advanced Materials* **2017,** *29* (31), 1700870.
17. Rogers, G. W.; Liu, J. Z., Monolayer graphene oxide as a building block for artificial muscles. *Applied Physics Letters* **2013,** *102* (2), 021903.
18. Rogers, G. W.; Liu, J. Z., High-performance graphene oxide electromechanical actuators. *Journal of the American Chemical Society* **2012,** *134* (2), 1250-1255.
19. Van Thanh, V.; Hung, N. T.; Van Truong, D., Charge-induced electromechanical actuation of Mo- and W-dichalcogenide monolayers. *RSC Advances* **2018,** *8* (67), 38667-38672.